A Letters Journal Exploring the Frontiers of Physics

December 2011

EPL, **96** (2011) 64001
doi: 10.1209/0295-5075/96/64001

www.epljournal.org

Stretch-induced wrinkles in reinforced membranes: From out-of-plane to in-plane structures

A. Takei[1(a)], F. Brau[2], B. Roman[1] and J. Bico[1]

[1] *Physique et Mécanique des Milieux Hétérogènes, CNRS UMR 7636, UPMC and University Paris Diderot, ESPCI-ParisTech - 10 rue Vauquelin, F-75231 Paris Cedex 05, France, EU*
[2] *Laboratoire Interfaces and Fluides Complexes, CIRMAP, Université de Mons - 20 Place du Parc, B-7000 Mons, Belgium, EU*

received 7 September 2011; accepted in final form 26 October 2011
published online 5 December 2011

PACS 46.32.+x – Static buckling and instability
PACS 46.70.De – Beams, plates, and shells
PACS 81.16.Dn – Self-assembly

Abstract – We study, through model experiments, the buckling under tension of an elastic membrane reinforced with a more rigid strip or fiber. In these systems, the compression of the rigid layer is induced through Poisson contraction as the membrane is stretched perpendicularly to the strip. Although strips always lead to out-of-plane wrinkles, we observe a transition from out-of-plane to in-plane wrinkles beyond a critical strain in the case of fibers embedded into elastic membranes. We describe through scaling laws the evolution of the morphology of the wrinkles and the different transitions as a function of material properties and stretching strain.

Wrinkled membranes. – Multi-layered systems composed of materials with contrasted elastic properties are ubiquitous in Nature and technology. Those systems are characterized by morphological instabilities when subjected to sufficiently large applied stress. Human skin as well as engineered materials are indeed prone to form wrinkles when compressed [1–3]. Although generally undesired, regular wrinkles observed on compressed thin films have been used for micro-patterning [4–6], to assess the magnitude of the forces acting on a cell wall [7] or to characterize material mechanical properties [8–10]. In flexible electronics systems, rigid circuits are also deposited on (or embedded into) elastomeric substrates. Fine controls of the buckling and the possible delamination of the circuit occuring when the matrix is deformed are then required [11–15]. While the formation of wrinkles on thick soft substrates entirely covered with an inextensible thin film has been extensively studied [10,16], less works have been devoted to localized reinforcement of soft membranes by strips or fibers [17–22], although these geometries are important for applications in stretchable electronics [11,23]. In this letter we propose to study the buckling under tension of elastic membranes reinforced with a rigid strip or fiber through model experiments spanning a wide range of physical parameters.

Our experimental setup is illustrated in fig. 1: a rubber sheet is stretched between a pair of parallel clamps displaced by a material testing machine (Instron). Previous studies have reported the formation of wrinkles when an elastic sheet is stretched beyond a critical strain, as a consequence of a mismatch between the width reduction due to Poisson effect and the fixed width at the clamps [1,24–26]. In contrast to what has been described in these studies, we do not observe spontaneous wrinkles when the rubber sheet is stretched within the range of strains selected for our experiments. However, we consider rubber sheets reinforced by a thin, more rigid, elastic strip adhering on its surface, or by a thin thread embedded inside the sheet. The strips or threads are placed perpendicular to the traction (fig. 1), and in this case we do observe wrinkles that extend over a finite area on the membrane (region R_2, fig. 1(a)). Similar wrinkles are also formed when a rubber balloon circumscribed by a stiff strip is deflated as demonstrated by Concha *et al.* [27]. In particular this system exhibits interesting non-linear patterns as the strain is progressively increased.

In the first part of the letter, we focus on the case of the reinforcement with a strip and describe, through scaling arguments, how the wavelength of the wrinkles depends on

(a) E-mail: atsushi.takei@espci.fr

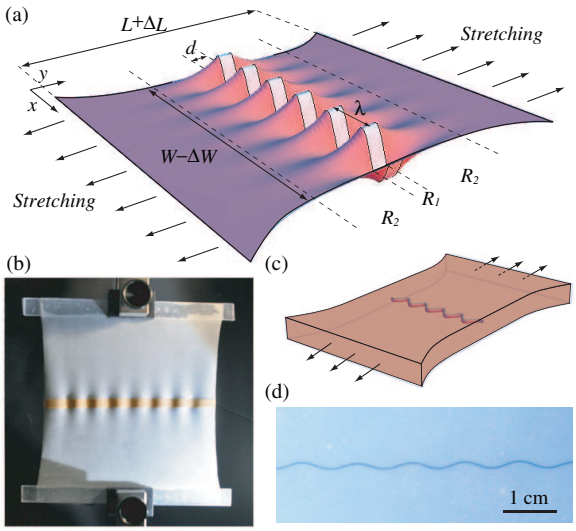

Fig. 1: (Colour on-line) (a) Sketch and (b) picture of the experimental setup: a soft sheet reinforced with a strip is stretched in the perpendicular direction to the strip, which induces the formation of out-of-plane wrinkles. If a thick membrane is reinforced with a fiber, the fiber buckles in the plane of the membrane: (c) sketch of the setup, (d) view of the of the in-plane wrinkles.

material properties, geometry and applied strain. We then compare these predictions with macroscopic experiments spanning a wide range of physical parameters. The second part is dedicated to the case of embedded fibers. We show that the stretch-induced undulation can also take place in the plane of the membrane, rather than out of the plane. We predict the wavelength of the in-plane wrinkles and give the condition under which this peculiar instability appears.

Reinforcement with a strip. – When a membrane of initial length L is stretched with a strain $\epsilon = \Delta L/L$ in the y-direction (fig. 1(a)), the Poisson effect induces a relative compressive strain $\nu_m\epsilon$ in the perpendicular direction x, where ν_m is the Poisson coefficient of the soft membrane. If the membrane is reinforced with an inextensible strip of width $d \ll L$, the strip may release the compressive stress by buckling out of the plane. The traditional linear stability analysis of the planar state would predict the exact value of the wavelength, but only at the threshold of instability [28,29]. Conversely, far from threshold analytical predictions describe the extension of the wrinkles [3] but not their wavelength. Here we choose to present scaling arguments, based on a minimization of the global elastic energy, to describe the evolution of the wavelength as the strain is increased.

We assume that the strip is inextensible and consider the energy in two complementary regions: bending energy $\mathcal{U}_1$ of the strip in the region R_1, stretching and bending energies $\mathcal{U}_2$ in the region R_2 where the membrane alone is deformed (fig. 1(a)). We first estimate the elastic energy

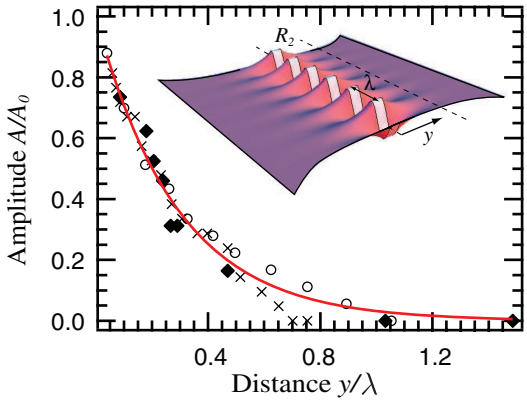

Fig. 2: (Colour on-line) Normalized amplitude of the wrinkles as a function of the relative distance from the borders of the strip y/λ. Circles (○): adhesive tape on rubber sheet, $h_m = 0.3\,\mathrm{mm}$, $\epsilon = 13.3\%$, $d = 10\,\mathrm{mm}$. Diamonds (◇): adhesive tape on rubber sheet, $h_m = 0.3\,\mathrm{mm}$, $\epsilon = 13.3\%$, $d = 2\,\mathrm{mm}$. Crosses (×): plastic fiber of radius 0.2 mm embedded in polyvinylsiloxane, $h_m = 2\,\mathrm{mm}$, $\epsilon = 13.3\%$. Full line: exponential fit, $A/A_0 = \exp(-3.4\,y/\lambda)$.

in region R_1: the bending energy of the strip is given by [28,29]

$$\mathcal{U}_1 \sim B\left(\frac{A}{\lambda^2}\right)^2 W d, \tag{1}$$

where λ and A are the respective wavelength and amplitude of the wrinkles, W the width of the membrane, and B the bending rigidity of the composite band formed by the actual rigid strip and the soft membrane. This effective stiffness B can be determined from material parameters using classical composite beam theory [10,14]. In the relevant limit for our experiments, the Young modulus of the rigid strip E_s is much larger than the modulus for the soft membrane E_m, whereas the thickness of the strip h_s is small compared to the thickness of the membrane h_m. The simplification of the general expression for the bending stiffness finally gives

$$B \simeq \frac{1 + m^2n^4 + 4mn}{1 + mn}\,\frac{E_m h_m^3}{12(1-\nu^2)}, \tag{2}$$

with $m = E_s/E_m$ $(m \gg 1)$ and $n = h_s/h_m$ $(n \ll 1)$ and where ν is an effective Poisson coefficient that we take arbitrarily equal to 0.5 in the following, a typical value for rubbery materials. Note that the stiffness of the composite band is dominated by the strip for $E_s h_s^2 \gg E_m h_m^2$.

We now turn to the elastic energy in region R_2, where the soft membrane is also deformed beyond the strip. The characteristic size of this region is expected to be proportional to λ as a consequence of the elliptic nature of elasticity equations [28,29]. Indeed, measurements of the normalized amplitude of the wrinkles as a function of the relative distance from the strip y/λ collapse on an exponentially decaying master curve (fig. 2). The corresponding decay length is found of the order of 0.3λ.

In addition to being bent, the membrane is also stretched in the R_2 region with a typical strain $(A/\lambda)^2$ due to excess in length imposed by the out-of-plane wrinkles. The deformation energy of the soft membrane in R_2 is thus given by the sum of bending and stretching energies $\mathcal{U}_2 = \mathcal{U}_{2b} + \mathcal{U}_{2s}$, with

$$\mathcal{U}_{2b} \sim E_m h_m^3 \left(\frac{A}{\lambda^2}\right)^2 \lambda W, \tag{3}$$

$$\mathcal{U}_{2s} \sim E_m h_m \left(\frac{A}{\lambda}\right)^4 \lambda W. \tag{4}$$

Since the strip is assumed to be inextensible, strain, amplitude and wavelength are geometrically related by $(A/\lambda)^2 \sim \Delta W/W$, which we take equal to $\nu\epsilon$. This last assumption is only valid in the limit $W \gg \lambda$. Indeed if the strip remained straight, the membrane should be perturbed on a large scale (of order W in the y-direction, similary to the distortion near the clamped boundary conditions), and its stretching energy $E_m h_m W^2 (\nu\epsilon)^2$ would thus be greater than the energy derived for $\mathcal{U}_{2s}$ for large values of W/λ. As a consequence, bending energies tend to favor large wavelengths ($\mathcal{U}_1 \propto \lambda^{-2}$ and $\mathcal{U}_{2b} \propto \lambda^{-1}$), whereas the stretching energy $\mathcal{U}_{2s} \propto \lambda$ is minimized when the wavelength vanishes. Note that the tension in the elongated direction provides another mechanism which tends to bring down amplitudes and wavelengths. The corresponding stretching energy indeed scales as $T(A/\lambda)^2 \lambda W$, where $T \sim Eh\epsilon$ is the applied tension. But the resulting expression for this energy thus follows the same scaling law as the stretching energy $\mathcal{U}_{2s}$ (eq. (4)) and no additional term is required.

The optimal wavelength is selected by the minimization of the total energy $\partial(\mathcal{U}_1 + \mathcal{U}_2)/\partial\lambda = 0$. Two successive regimes can be identified. For small strains, the wavelength is governed by the balance between bending and stretching energies of the membrane alone:

$$\lambda \sim h_m \, (\nu\epsilon)^{-1/2}. \tag{5}$$

Interestingly the main role of the strip is, in this first regime, to impose the inextensibility condition. The predicted wavelength is indeed independent of the material properties of the band.

For larger deformations, *i.e.* larger strains, the bending energy of the strip dominates over the bending energy of the membrane, leading to the wavelength

$$\lambda \sim \left(\frac{Bd}{E_m h_m}\right)^{1/3} (\nu\epsilon)^{-1/3}, \tag{6}$$

which corresponds to the regime described in ref. [27].

The crossover between these two regimes occurs when the two bending energies, $\mathcal{U}_1$ and $\mathcal{U}_{2b}$, are of the same order of magnitude. The wavelength λ_0, obtained from this balance of energy, and the strain ϵ_0, obtained from eq. (5) or (6) using $\lambda = \lambda_0$, characterizing the transition between these two regimes are thus

$$\lambda_0 \sim Bd/E_m h_m^3 \quad \text{and} \quad \nu\epsilon_0 \sim (E_m h_m^4/Bd)^2. \tag{7}$$

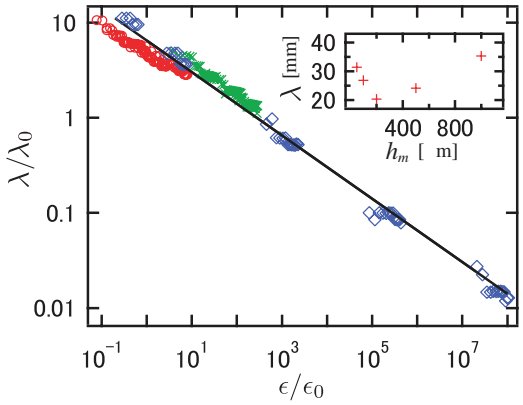

Fig. 3: (Colour on-line) Normalized wavelength of wrinkles observed on membranes reinforced with a strip. (×) Natural latex ($E_m = 1.5$ MPa), (◇) silicone rubber ($E_m = 3$ MPa) and (○) polyvinylsiloxane ($E_m = 0.15$ MPa) with thicknesses ranging from 50 μm to 1.8 mm were selected for the soft membrane. Strips were cut from a plastic sheet with a thickness of 15 μm or commercial adhesive tapes of Young modulus $E_s \simeq 1$ GPa. Each symbol corresponds to the same material system. Full line: scaling law $\lambda/\lambda_0 = 6.0\,(\epsilon/\epsilon_0)^{-1/3}$ (eq. (6)). Inset: non-monotonic behavior of λ with respect to h_m as the other parameters are maintained constant ($E_s/E_m = 400$).

These transition values for the wavelength and for the strain are used without any prefactor to normalize the experimental data. The first regime is now described by $\lambda/\lambda_0 \sim (\epsilon/\epsilon_0)^{-1/2}$, whereas the second regime obeys $\lambda/\lambda_0 \sim (\epsilon/\epsilon_0)^{-1/3}$. The expected evolution of the wavelength of this system contrasts from the case of a plain rigid sheet or even a thin ribbon deposited on a thick soft substrate [6,8–10,16,18] or at the surface of a liquid [30] under uniaxial compression, where the wavelength of the wrinkles does not depend on the applied strain. Indeed this last situation corresponds to $\lambda \gg h_m$ and considering the bending of the membrane would not be relevant.

The experiments conducted through a broad range of material parameters ($10^{-9} < \epsilon_0 < 0.5$, $0.1 < \epsilon/\epsilon_0 < 10^8$, 3.5 mm $< \lambda_0 <$ 2000 mm and $0.01 < \lambda/\lambda_0 < 10$) are in very good agreement with the second regime over 9 orders of magnitude (fig. 3). Note the non-monotonic variation of λ with the thickness h_m of the membrane when all other parameters are kept constant. Indeed, we expect the bending stiffness of the composite system, B to be dominated by the bending stiffness of the strip, $E_s h_s^3$, for low values of h_m and by the bending stiffness of the membrane, $E_m h_m^3$, for larger values. Increasing the thickness of the membrane between these extreme cases yields a non-monotonic transition for the wavelength from $\lambda \sim h_m^{-1/3}$ to $\lambda \sim h_m^{2/3}$ (see eq. (6)). This transition is observed in the inset in fig. 3.

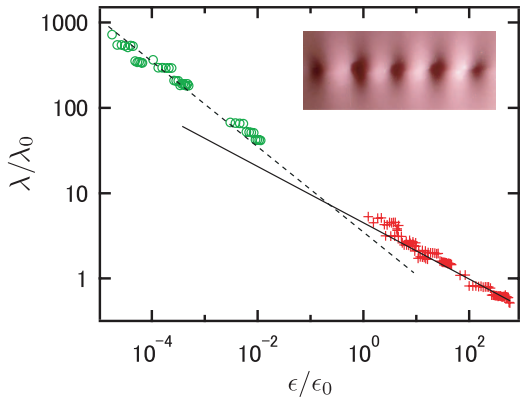

Fig. 4: (Colour on-line) Normalized wavelength of the wrinkles observed on membranes reinforced with a fiber (out-of-plane buckling). D, h_m, E_f and E_m range, respectively, from 0.07 to 5 mm, 1 to 2.3 mm, 2 to 290 GPa and 0.05 to 0.35 GPa. Dashed line and full line: scaling laws $\lambda/\lambda_0 = 3.5\,(\epsilon/\epsilon_0)^{-1/2}$ (for $\epsilon/\epsilon_0 \ll 1$) and $\lambda/\lambda_0 = 5.0\,(\epsilon/\epsilon_0)^{-1/3}$ (for $\epsilon/\epsilon_0 \gg 1$) corresponding to eqs. (5) and (6), respectively. Inset: close-up view of the out-of-plane wrinkles of a fiber.

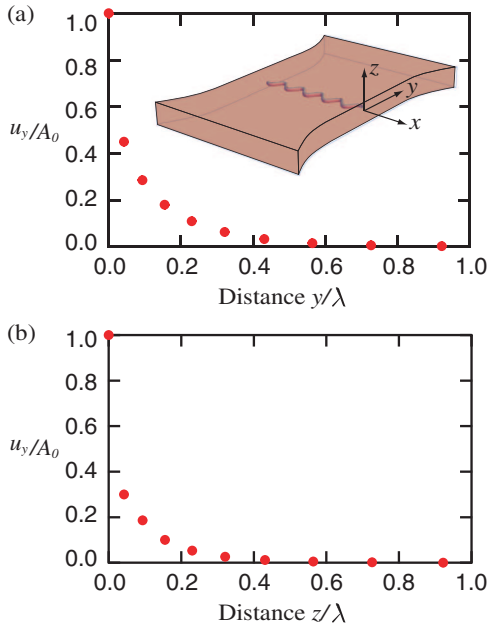

Fig. 5: (Colour on-line) The displacement along the y-direction u_y is plotted as a function of y (panel (a)) and z (panel (b)). The values of y and z are normalized by λ, and the amplitude of the deformation u_y is normalized by A_0.

Obtaining data for strips in the first regime described by eq. (5) is however difficult in practice since it would correspond to strains that are below the resolution of our experimental setup ($\epsilon_{min} \sim 0.5\%$). Larger values of ϵ_0 can nevertheless be obtained by decreasing d, *i.e.*, by selecting narrower strips or even rods. In order to assess the first regime, experiments were conducted with fibers embedded into soft membranes obtained by cross-linking liquid polyvinylsiloxane (Elite double from Zhermack). As in the case of strips, out-of-plane wrinkles are observed with relatively thin membranes (fig. 4). The arguments developed for a strip of width d can indeed be easily adapted to a fiber of diameter D by replacing, in eq. (6), the bending stiffness Bd by the bending rigidity of the fiber $\frac{\pi}{64} E_f D^4$ for $E_f \gg E_m$. As illustrated in fig. 4, the experimental results are in good agreement with the theoretical predictions over a range in ϵ/ϵ_0 spanning 8 orders of magnitude, this time reaching the first regime.

In-plane buckling. – Exploring this first regime further down requires thinner fibers. However a new feature is observed as the ratio h_m/D is increased: the fiber buckles in the plane of the membrane (fig. 1(d)). Considering the bending of the membrane is thus no longer relevant. As a matter of fact, the elastic material is compressed (and stretched) along the buckled fiber with a typical displacement A and a radial extension ℓ, leading to a characteristic strain $\epsilon \sim A/\ell$. Similarly to the 2D case previously described, we expect ℓ to be proportional to the wavelength λ. Due to the difficulty to measure directly the strain through the membrane, we conducted numerical simulations based on the finite-element method (Cast3M software) to estimate how the elastic material is deformed. In the simulation, the in-plane oscillations of the fiber are modeled as an imposed displacement in the y-direction $u_y = A_0 \sin(2\pi x/\lambda)$ at $y = 0$ and $z = 0$ (see fig. 5(a)). Within the limit of linear elasticity used for these simulations, the final strain is always proportional to A_0. The boundary conditions were λ-periodic in the x-direction, and the other dimensions of the thick membrane were chosen as 25λ and 10λ in the y- and z-direction, respectively. The displacement in the y-direction is plotted in fig. 5 as a function of the normalized directions y/λ and z/λ for $x = \lambda/4$ (maximum deformation). The displacement is found to vanish as the distance from the fiber exceeds 0.2λ. We finally verified that varying the Poisson ratio from 0.1 to 0.5 did not lead to any significant modification of the distribution of strains.

The stretching energy of the membrane finally reads

$$\mathcal{U}_{3s} \sim E_m W \lambda^2 \left(\frac{A}{\lambda}\right)^2 \sim E_m W A^2, \tag{8}$$

where we have assumed that the strained zone is smaller than the thickness of the membrane ($0.2\lambda \ll h_m$, as indicated by the numerical simulation). The bending energy of the fiber is simply given by $\mathcal{U}_{1f} \sim E_f D^4 W (A/\lambda^2)^2$. Minimizing the global energy $\mathcal{U}_{1f} + \mathcal{U}_{3s}$ with respect to λ finally prescribes the wavelength of the buckles:

$$\lambda \sim D(E_f/E_m)^{1/4}, \tag{9}$$

which is similar to the expression derived by Ryu and Xiao *et al.* for the buckling of Si nanowires [21,22]. This relation is in good agreement with the experimental data

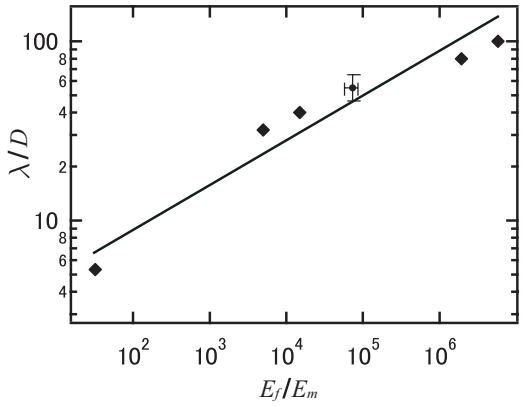

Fig. 6: In-plane buckling of fibers embedded in thick membranes. D, h_m, E_f and E_m range, respectively, between: 0.05 and 0.47 mm, 4 and 8 mm, 1 MPa and 290 GPa, 0.05 and 0.15 MPa. Full line: scaling law $\lambda/D = 2.8\,(E_f/E_m)^{1/4}$ corresponding to eq. (9). Dot symbol: data extracted from [21].

obtained for a ratio E_f/E_m spanning over 6 orders of magnitude (fig. 6). We added a data point extracted from reference [21] where close experiments have been carried with silicon nanowires deposited on elastomeric substrates[1]. Note finally that our result is very close to the classical problem of a substrate uniformly covered with a thin layer where the wavelength is independent of the load. The exponents are however different because of the difference in the geometry ($\lambda \sim h(E_s/E_m)^{1/3}$ in the case of the thin film [9]).

The in-plane buckling only exist if $\lambda \ll h_m$, which gives the following necessary condition:

$$D \ll h_m (E_m/E_f)^{1/4}, \tag{10}$$

which only holds for thin fibers embedded into thick enough membranes, as it is observed experimentally (the quantity $(D/h_m)(E_f/E_m)^{1/4}$ typically ranges between 0.12 and 0.34 in our experiments).

The transition between out-of-plane and in-plane buckling modes can be predicted by comparing the elastic energy of the two modes. These energies are simply derived by using the estimated wavelengths in the expressions for the energies. For a given strain ϵ, the elastic energy for the in-plane mode is thus given by $\mathcal{U}_{in} \sim (E_f E_m)^{1/2} D^2 W \nu\epsilon$. The elastic energy for the out-of-plane buckling when $\epsilon \ll \epsilon_0$ is given by $\mathcal{U}^I_{out} \sim E_m h_m^2 W(\nu\epsilon)^{3/2}$. In-plane buckling is expected when $\mathcal{U}_{in} < \mathcal{U}^{I,II}_{out}$, which corresponds to an applied strain larger than a critical value:

$$\nu\epsilon > \nu\epsilon_{ip} \sim (D/h_m)^4 E_f/E_m, \tag{11}$$

which is consistent with the assumption $\epsilon_{ip} \ll \epsilon_0$. In the second regime corresponding to $\epsilon \gg \epsilon_0$, we find $\mathcal{U}^{II}_{out} \sim (E_m h_m)^{2/3}(E_f D^4)^{1/3} W(\nu\epsilon)^{5/3} \gg \mathcal{U}_{in}$ if the condition (10) remains valid, which favors in-plane buckling. As a result, in-plane buckling inevitably appears above a critical strain ϵ_{ip} if the fiber is thin enough compared to the thickness of the membrane.

[1]In this case, the deformed volume in the substrate is expected to be one half of the embedded case, which would lead to a correction of order $2^{1/4} \simeq 1.2$ for the wavelength.

Conclusion. – In summary, membranes reinforced with rigid strips or fibers are found to buckle when stretched uniaxially in a direction perpendicular to the embedded structures. As the strain is increased, two successive regimes are predicted depending on the relative bending energy stored in the soft membrane and in rigid structure. In contrast to the case of a confined rigid sheet resting on a soft substrate, the wavelength depends on the applied strain ($\lambda \propto \epsilon^{-1/2}$ and $\epsilon^{-1/3}$, respectively). These theoretical scaling laws are in good agreement with experiments conducted over a wide range of experimental parameters. In addition, a non-intuitive regime of in-plane buckling is found with fibers embedded into a thick membrane. In this configuration the wavelength only depends on the material parameters but not on the applied strain. We expect our results to be relevant for designing stretchable electronic devices or more generally composite materials where the formation of buckles can be crucial. Measuring the wavelength of the wrinkles may also be used in metrology as a way of inferring the strain applied to a membrane in minute samples where conventional methods are not applicable.

* * *

This study was partially funded by the ANR project MecaWet, the Japan Society for the Promotion of Science and the Government of the Region of Wallonia (REMANOS Research Programme). We thank J. Hure for his numerical simulations of the problem.

REFERENCES

[1] Cerda E. and Mahadevan L., *Phys. Rev. Lett.*, **90** (2003) 074302.
[2] Cerda E., *J. Biomech.*, **38** (2005) 1598.
[3] Stein M. and Hedgepeth J. M., Nasa TN D-813 (1961).
[4] Chan E. P. *et al.*, *Adv. Mater.*, **20** (2008) 711.
[5] Ohzono T. *et al.*, *Soft Matter*, **5** (2009) 4658.
[6] Chiche A., Stafford C. M. and Cabral J. T., *Soft Matter*, **4** (1997) 2360.
[7] Burton K. and Taylor D. L., *Nature*, **385** (1997) 450.
[8] Bowden N. *et al.*, *Nature*, **393** (1998) 146.
[9] Stafford C. M. *et al.*, *Nat. Mater.*, **3** (2004) 545.
[10] Chung J. Y., Nolte A. J. and Stafford C. M., *Adv. Mater.*, **23** (2011) 349.
[11] Khang D. Y. *et al.*, *Science*, **311** (2006) 208.
[12] Sun Y. *et al.*, *Adv. Mater.*, **18** (2006) 2857.
[13] Sun Y. and Rogers J. A., *J. Mater. Chem.*, **17** (2007) 832.
[14] Kim D.-H. *et al.*, *Science*, **320** (2008) 507.
[15] Rogers J. A., Someya T. and Huang Y., *Science*, **327** (2010) 1603.
[16] Brau F. *et al.*, *Nat. Phys.*, **7** (2011) 56.

[17] Jiang C. *et al.*, *Nano Lett.*, **6** (2006) 2254.
[18] Jiang H. *et al.*, *Proc. Natl. Acad. Sci. U.S.A.*, **104** (2007) 15607.
[19] Gunawidjaja R. *et al.*, *Chem. Mater.*, **19** (2007) 2007.
[20] Xiao J. *et al.*, *J. Appl. Phys.*, **104** (2008) 033543.
[21] Ryu S. Y. *et al.*, *Nano Lett.*, **9** (2009) 3214.
[22] Xiao J. *et al.*, *Nanotechnology*, **21** (2010) 085708.
[23] Khang D. Y. *et al.*, *Nano Lett.*, **8** (2008) 124.
[24] Friedl N., Rammerstorfer F. G. and Fisher F. D., *Comput. Struct.*, **78** (2000) 185.
[25] Cerda E., Ravi-Chandar K. and Mahadevan L., *Nature*, **419** (2002) 579580.
[26] Puntel E., Deseri L. and Fried E., *J. Elast.*, **105** (2011) 137.
[27] Concha A. *et al.*, *Phys. Rev. E*, **75** (2007) 016609.
[28] Timoshenko S., *Theory of Plates and Shells* (McGraw-Hill) 1964.
[29] Landa L. D. and Lifshitz E. M., *Theory of Elasticity* (Pergamon) 1986.
[30] Pocivavsek L. *et al.*, *Science*, **320** (2008) 912.